Research Article

Journal of Environmental Nanotechnology

Green Synthesis and Characterization of Nickel Nanoparticles using Aqueous Extract of *Moringa oleifera* Flower

C. F. Simple Lotus[1*], Jino John[2], S. Ramesh Kumar[3]

[1]Stella Maris Institute of Development Studies, Kanyakumari, TN, India

[2]Department of Botany and Biotechnology, Emmanuel College, Vazhical, Kudappanamoodu, KL, India

[3]Research Department of Zoology, Sadakathullah Appa College, Manonmaniam Sundaranar University, Abishekapatti, Tirunelveli, TN, India

Received: 04.02.2023 Accepted: 17.02.2023 Published: 30-03-2023

*simplelotus@gmail.com

ABSTRACT

An attempt has been made in this work to green synthesize nickel nanoparticles using the aqueous flower extract of *Moringa oleifera*, a common plant in which all parts are edible and rich in iron content, through the biosynthesis method. The synthesized *Moringa oleifera* flower extract nanorods were characterized by UV–Vis. spectroscopy, Fourier Transform Infrared spectroscopy, X-Ray Diffraction analysis and Transmission Electron Microscopy. In addition, the antimicrobial activity of the nanorods was evaluated. The nanorods were found to be crystalline in nature with rod-like structures having a mean particle size of 35 nm.

Keywords: Green Synthesis; Nickel; Nanoparticles; *Moringa oleifera*.

1. INTRODUCTION

Research in the field of nanotechnology plays a pivotal role in the expanse of contemporary science and technology. The behaviour of the material can be enhanced through nano size which provides improved function. Nanostructure metals has prominent applications in sensors, catalysis, electronics, biomedicine and biotechnology. In this nanotechnology world, one of the key concerns is the potential impact of nanoparticles on the surroundings. The collaboration of nanoparticles with natural resources leads to a novel nanostructured material with controlled shape, size, roughness, surface coatings and surface chemistry (Das *et al.* 1994). The appearance of transferable syndrome causes a severe danger to public health, particularly with the emergence of antibiotic-resistant bacterial strains. Gram-negative and gram-positive pathogens are considered to majorly threaten public health. Antibiotics and biological materials have been used to control infections. For these reasons, the interest in green synthesized metal nanoparticles (MNPs) is increasing. Nickel nanoparticles (Ni-NPs) are mostly used in biotechnology and medical fields. The formation of small nanoparticles with proper stability and distribution is vital for active and efficient nanoparticles (Fahey, 2005). These nanoparticles present strong antimicrobial activity at low concentrations. Antibacterial agents have a huge impact on water disinfection, textiles, packaging, construction, food and medicine. The interaction of biosynthesized MNPs with pathogenic microorganisms plays the lowest level in the food chain of the atmosphere. Ni-NPs have been extensively studied due to their unique photo-thermal, optical and electrical properties. Ni-NPs as well as metallic Ag or Ag ions are used in medicine for dental materials, water treatment, textile fabrics, sunscreen lotions, burn treatment, etc. They provide high thermal stability, low volatility and small toxicity to human cells, Ni-NPs are accounted to acquire effective antiplatelet, antifungal, antiviral antimicrobial agent and anti-inflammatory characteristics against different pathogens. Nowadays, green synthesis of Ni-NPs has attracted great interest, owing to the increasing requirement to develop uncontaminated and harmless substances, renewable materials and eco-friendly solvents. In recent years, extracts of pomegranate peel, stems and leaves of *Hibiscus cannabinus*, beetroot, fenugreek, *Kalanchoe daigremontiana*, *Acalypha hispida and Amorphophallus paeoniifolius* were found appropriate for the synthesis of Ni-NPs (Inbathamizh and Padmini, 2003).

On the other hand, Moringa flowers received little attention of researchers in spite of their significant nutritional and traditional healing properties. 'Muringa Poovuthoran' is a tasty and seasonal dish of Keralites in India, made from Moringa flowers. In other parts of world too, flowers are the favorite ingredients of various dishes such as lasagna, omelettes, soups, sea foods, pasta dishes, pizza, etc.; they are eaten raw as in salads or used for making tea and honey. Bhavaprakasha, an important treatise on Ayurveda, depicts Shigru flowers (Moringa flowers) as a wholesome food for healthy eyes. (Koul and Chase, 2005) Anwar *et al.* made a concise presentation of common medicinal uses of different parts of *Moringa oleifera* which included an impressive list to flower alone for its high medicinal value as a stimulant, aphrodisiac, abortifacient and cholagogue. (Molina *et al.* 2019) This study starts with a short description on morphology and anatomy of the flowers, major phytochemicals present and compounds identified and isolated. Bioassays of flowers conducted using different extracts are then presented in a tabular form so as to make an easy assessment on the pharmacogenetic prospects of the flower.

Flowers are fragrant yellowish white and bisexual, born in 10 to 25 cm long axillary, compound inflorescence called panicles. (Bindhu and Umadevi, 2013; Bindhu *et al.* 2020) Individual flowers, slightly zygomorphic, have dimensions of about 1 cm length by 2 cm breadth set in a basal cup of thalamus namely hypanthium. Sepals and petals are five in numbers, free, unequal, reflexed and spathulate. Stamens, five in number, are dorsifixed filaments of different lengths with posterior ones longer with yellow one-celled anther bending downwards. There are five staminodes alternating with the stamens forming an outer whorl. The gynoecium is tricarpellary syncarpous borne on a small gynophore. The ovary continues into a long style which protrude out of anthers and end in creamy white and pitted stigma (Selvakumar *et al.* 2018). Reports indicate a pollen presentation mechanism (Molina *et al.* 2019; Selvakumar *et al*. 2019; Deenanath and Evanie, 2014; Cheng *et al.* 2016). There are two peaks of flowering – the October-November rainy season and the April-May summer season.

2. EXPERIMENTAL DETAILS

2.1 Materials

Moringa oleifera flowers (MOF), shown in Fig. 1, were picked freshly from the garden of Stella Maris Institute Development Studies (SMIDS) Kanyakumari, Tamilnadu, India. Analytical grade of ($Ni(NO_3)_2\ 6H_2O$) were collected from Sigma Aldrich Chemicals, Tirunelveli, India.

2.2 Preparation of MOF Extract

At 120 ºC, 20 g of cleaned flowers were heated in distilled water. Then the extract was isolated by centrifugation for 10 min to remove unsolved parts (Deenanath, 2014); at the end of the process, a light-yellow extract was obtained after filtering through the filter paper.

Fig. 1: ***Moringa oleifera*** **flower**

2.4 Characterization of Ni-NPs

The optical studies of D2, D4, D6 and D8 solutions were characterized by Double Beam UV-visible Spectrophotometer in the 400–800 nm range. Then the samples were dried at 100 ºC and used for different characterization methods such as TEM, XRD and FTIR. Vibrational studies of flower extract were examined by using FTIR. Structural analysis of flower extract was made by X-ray Diffractometer with CuKα radiation = 1.5406 A˚. Morphology analysis was examined using a JEOL TEM 2010 HRTEM. Antimicrobial studies were observed by Disc diffusion method.

3. RESULTS AND DISCUSSION

3.1 Optical Studies

The optical properties of the nanoparticles were recorded with respect to high purity, and their crystallinity were confirmed with the help of Ultraviolet - Diffuse Reflectance Spectroscopy (UV-DRS) by observing an excitonic absorbance band at 300 nm with the tail extending towards a longer wavelength due to their quantum size effects, as shown in Fig. 2. The absorption peaks exhibit a broad peak due to the particle size. The stability of Ni-NPs can be attributed to their symmetrical polarity structure, which depends on the weak interaction of Van der Waals forces within the particle regime.

3.2 FTIR

Fig. 3 shows the FTIR spectra of Ni-NPs. FTIR absorption band in the range of 4000-400 cm^{-1} can be assigned to the vibration of ions in the crystal lattice, recorded using K-Br disc method; the peaks at 570.93 cm^{-1} correspond to the vibration of Ni in the octahedral hole and 663.51 cm^{-1} to the stretching vibrations in the Co^{2+} in the tetrahedral hole, showing the presence of single-phase face-centred cubic structured nanoparticles. Annealing at 500 ºC for two hours resulted in the change from amorphous to crystalline state with narrow particle size distribution with well-defined particle size, shape and phase purity.

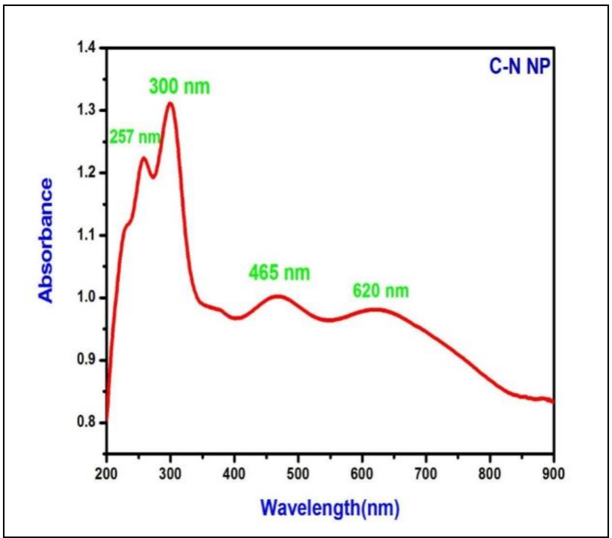

Fig. 2: UV- DRS of Ni-NPs

A stretching frequency at 3388 cm^{-1} and a weak asymmetric band at 1443 cm^{-1} support the presence of OH- group due to the absorption of water by nanoparticles during the sample preparation. The presence of two strong M-O stretching and bending frequencies at 663.51 cm^{-1} and 570.93 cm^{-1}, respectively, supports the presence of phase purity (monodispersed) in the face-centered cubic structure. A stretching frequency at 3788 cm^{-1} can be assigned to the presence of the amino group of proteins and a stretching frequency at 1788 cm^{-1} to the carbonyl group of flavonoids and other biomolecules.

3.3 XRD

X-ray diffraction pattern of the as-synthesized nickel nanopowder was analyzed to investigate the phase structure along with its crystallinity as illustrated in Fig. 4. This shows a crystalline structure with 8 peaks. The XRD pattern shows a significant amount of line broadening, which is a characteristic of nanoparticles. The XRD pattern exhibits prominent peaks at 19, 21.4, 23.26, 31.23. 35.1, 36.84, 44. 62 and 65.12°. The peak positions appearing at 2θ = 19, 23.26, 31.23, 35.1, 36.84, 44. 62 and 65.12° can be readily indexed as (111), (220), (311), (222), (220), (400) and (440) crystal planes The peaks were indexed to pure phase with a face-centered cubic structure, which correspond to JCPDS file (76–1802) after annealing the sample and by matching Bragg reflection peaks. The Ni ($3d^7$) located at tetrahedral and octahedral sites crystallizes in a spinel configuration. The average particle size calculated with the help of Debye-Scherrer equation was found to be 46 nm.

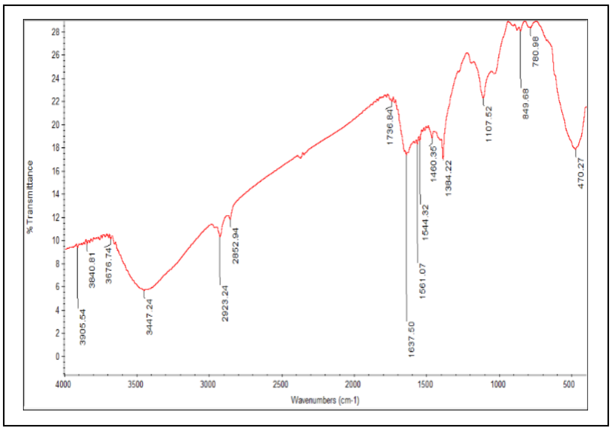

Fig. 3: FTIR images of Ni-NPs

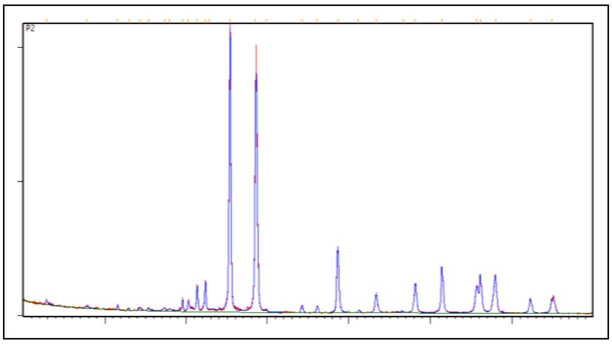

Fig. 4: XRD image of Ni-NPs

3.4 TEM

The surface morphological features of synthesized nanoparticles were studied by TEM. The image, shown in Fig. 5, reveals the microcrystalline nature of the particle after calcination with the least degree of agglomeration. Particles seem to have an irregular shape with chemical homogeneity with uniform morphology due to the presence of interparticle surface connectivity. It was observed that the annealing temperature increases the crystalline nature of the particle that changes due to nucleation. The nanoparticles were nanorod-shaped. The microstructural characterization studies were used to determine the size of nanoparticles and examine the homogeneity and size distribution.

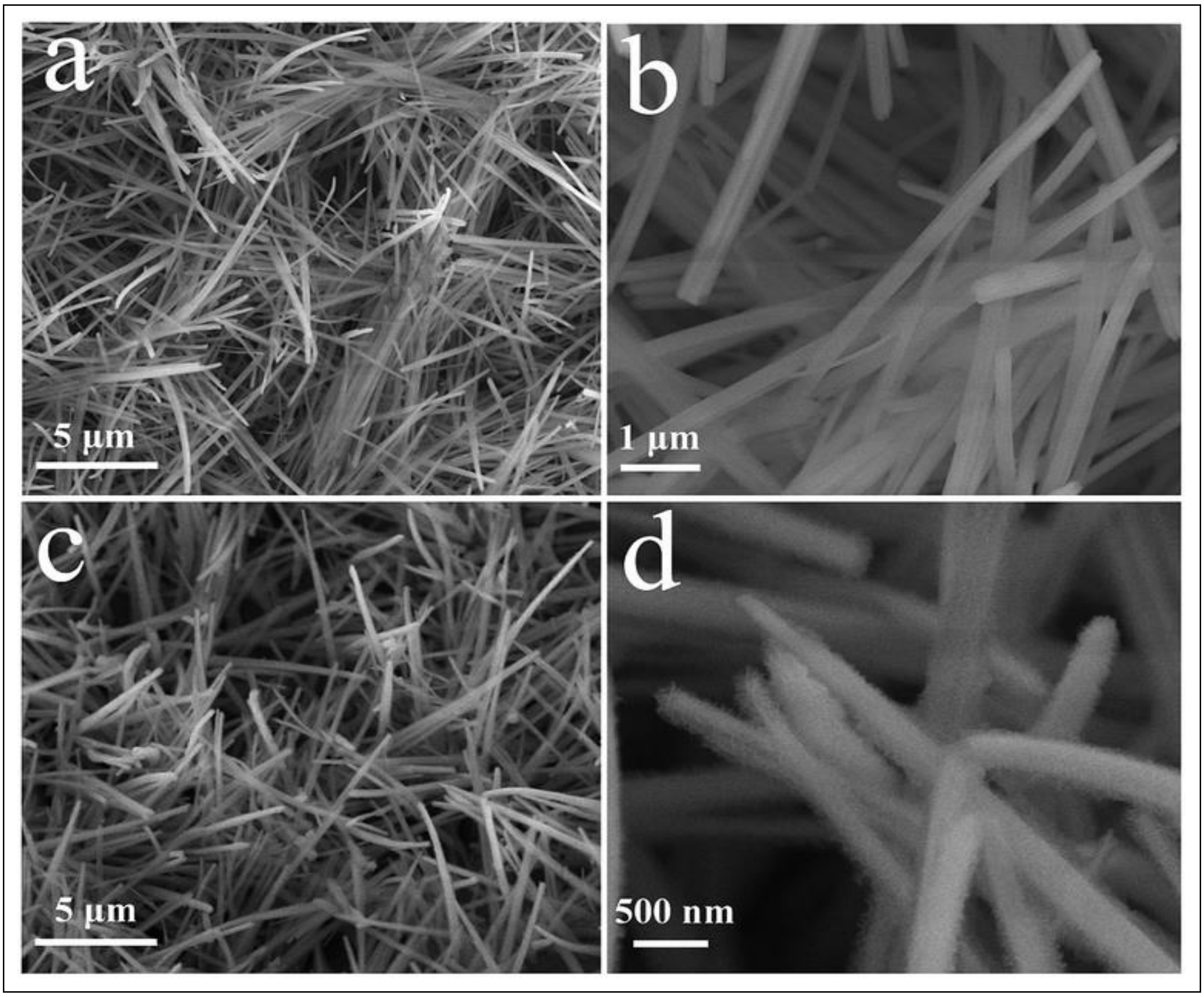

Fig. 5: TEM images of Ni-NPs

4. CONCLUSION

Flowers of *Moringa oleifera*, a previously unexplored part of the otherwise hugely investigated plant, is a warehouse of valuable bioactive phytochemicals. Preliminary investigations into the antibacterial characteristics of various solvent extracts are highly promising. There is scope for detailed studies to elucidate the mechanism behind the significant therapeutic potential of the Moringa flower as well as to isolate, purify and characterize the bioactive phytochemicals.

FUNDING

This research received no specific grant from any funding agency in the public, commercial, or not-for-profit sectors.

CONFLICTS OF INTEREST

The authors declare that there is no conflict of interest.

5. REFERENCES

Bindhu, M. R., Umadevi, M., Galal, A. E., Naif A. A., Mariadhas, V. A., Green synthesis and characterization of silver nanoparticles from Moringa oleifera flower and assessment of antimicrobial and sensing properties, *J. Photochem. Photobiol.*, B, 205, 111836 (2020). https://doi.org/10.1016/j.jphotobiol.2020.111836

Bindhu, M. R., Umadevi, M., Green synthesized gold nanoparticles as a probe for the detection of Fe^{3+} ions in water, *J. Clu. Sci.*, 25(4), 969-978 (2013). http://dx.doi.org/10.1007%2Fs10876-013-0679-8

Das, B. R., Kurup, P. A., Narasimha R. P. L., Ramaswamy, A. S., Antibiotic principle from *Moringa pterygosperma*, Naturwissenschaften, 41, 66-66 (1954). https://doi.org/10.1007/BF00634183

Deenanath, Evanie D., Production and characterization of bioethanol derived from cashew apple juice for use in internal combustion engine, Diss. University of the Witwatersrand, Faculty of Engineering and the Built Environment (2014).

Fahey, J. W., Moringa oleifera: A Review of the Medical Evidence for Its Nutritional, Therapeutic, and Prophylactic Properties. Part 1, Trees for Life Journal, 1(5), 1-15 (2005). https://doi.org/10.1201/9781420039078.ch12

Huining, C., Mingxiao, W., Yang, T., Yanzhi, S., Yongmei, C., Pingyu, W., Fabrication of NiOOH/Ni (OH) 2@ C electrode for detecting blood glucose by composited plating method, *Int. J. Electrochem. Sci.*, 11, 6085-6094 (2016). https://doi.org/10.20964/2016.07.24

Inbathamizh, L., Padmini, E., Effect of geographical properties on the phytochemical composition and antioxidant potential of Moringa oleifera flowers, BIOMEDRX, 1(3), 239-47 (2013).

Koul, B., Chase, N., Moringa oleifera Lam.: Panacea to several maladies, *J. Chem. Pharm. Res.*, 7(6), 687-707 (2015).

Molina, G. A., Esparza, R., LuisLópez-Miranda, J., Hernández-Martínez, A.R., España-Sánchez, B.L., Elizalde-Peña, E.A., Estevez, M., Green synthesis of Ag nanoflowers using Kalanchoe Daigremontiana extract for enhanced photocatalytic and antibacterial activities, *Colloids Surf.*, 180, 141-149 (2019). https://doi.org/10.1016/j.colsurfb.2019.04.044

Selvakumar, P., Sithara, R., Viveka, K., Sivashanmugam, P., Green synthesis of silver nanoparticles using leaf extract of Acalyphahispida and its application in blood compatibility, *J. Photochem. Photobiol B.*, 182, 52-61 (2018). https://doi.org/10.1016/j.jphotobiol.2018.03.018